Research Paper

Volume : 3 | Issue : 12 | December 2014 • ISSN No 2277 - 8179

Particle Size Determination And Morphological Study Of Nano Crystalline Ceramic Superconductor $La_{0.1}ZrY_{0.9}BaCa_2Cu3O_{4.5+x}$ At Three Different Temperatures

Physics

KEYWORDS : Lanthanum Zirconium Yttrium Barium Calcium Copper Oxide $La_{0.1}ZrY_{0.9}BaCa_2Cu3O_{4.5+x,}$ high temperature superconductors, XRD, SEM

Anitha S. Nair — Department of Physics, D.B College, Parumala, Kerala, India.

Jayakumari Isac — Centre for Condensed Matter, Department of Physics, CMS College, Kottayam, Kerala, India.

ABSTRACT

Today we are familiar with a large series of "high temperature superconductors" based on the ceramic materials with layers of Copper-oxide spaced by layers containing Barium and other atoms. Most of these type super conductors containing yttrium compounds, it has a regular crystal structure while the Lanthanum version is classified as a solid solution. Here author calculated the particle size of the superconductor Lanthanum Zirconium Yttrium Barium Calcium Copper Oxide ($La_{0.1}ZrY_{0.9}BaCa_2Cu3O_{4.5+x,}$) at different treating temperatures. It was prepared by the solid state reaction method via a high-energy ball milling process through mechanically assisted synthesis and calcined in a specially designed high temperature furnace. Here the authors characterized the sample by X-ray Diffraction (XRD), SEM and EDX. The structure of this material is found to be orthorhombic and is confirmed from the XRD results with JCPDS files and XPERT-PRO software, while a≠b≠c and α=β=γ=900. The particle size determination by the XRD analysis with Debye Scherrer's formula, SEM, instrumental broadening and Williamson-Hall Plot method confirmed that the sample's particle size is less than 100 nm.

INTRODUCTION

Ceramics can withstand very high temperatures such as temperatures that range from 800°C to 1,600°C.Ceramic materials are brittle, hard, strong in compression, weak in shearing and tension. They withstand chemical erosion that occurs in an acidic or caustic environment. Also withstanding erosion from the acid and bases applied to it. At low temperatures, La_2O_3 has an A-M2O3 hexagonal crystal structure. The La_{3+} metal atoms are surrounded by a 7 co-ordinate group of O_2-atoms, the oxygen ions are in an octahedral shape around the metal atom and there is one oxygen ion above one of the octahedral faces Yttrium oxide Y2O3 nanoparticle is an air-stable, solid substance. In this work the authors describe the preparation of $La_{0.1}ZrY_{0.9}BaCa_2Cu_3O_{4.5+x}$ ceramic material and characterized to show good quality, homogeneity and the desired non stoichiometry of the sample prepared. The results were analyzed by X-ray diffraction (XRD), SEM, EDX. The particle size was determined from XRD details by Debye Scherrer formula. The SEM studies revealed that its particle size is in hundred nanometer range. The EDX spectrum of $La_{0.1}ZrY_{0.9}BaCa_2Cu_3O_{4.5+x}$ gave the information on the elemental composition of the material. Instrumental Broadening and Williamson-Hall Plot method utilized to found the particle size and strain of the material.

2. Materials and Experimental Methods

$La_{0.1}ZrY_{0.9}BaCa_2Cu_3O_{4.5+x}$ has perovskite structure. The perovskite structure is adopted by many oxides. The representative structure of perovskite compounds is cubic, the compounds in this family may possess or undergo some distortion. The orthorhombic and tetragonal phases are most common variants. Figure.1 shows the structure of $La_{0.1}ZrY_{0.9}BaCa_2Cu_3O_{4.5+x}$ and T_C of some related high temperature superconductor materials.

Lanthanum-doped ceramics with the chemical formula $La_{0.1}ZrY_{0.9}BaCa_2Cu_3O_{4.5+x}$ was prepared by the solid state thermochemical reaction technique. For the Sample preparation reagent grade chemicals of high purity (99.99%) Lanthanum oxide, Zirconium oxide, Yttrium oxide, Barium carbonite, Calcium oxide and Copper oxide powders were used as the raw materials and weighed according to their molecular formula.

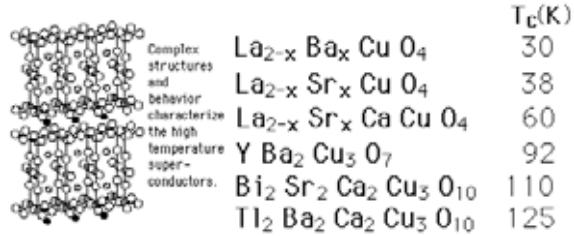

Figure.1 Structure of $La_{0.1}ZrY_{0.9}BaCa_2Cu_3O_{4.5+x}$

The powders of the required ceramics were mixed mechanically. Mechanical mixing is usually done by hand mixing in agate mortar for very long time. Then ball milled with suitable balls for long time to insure homogeneity and attrition milling. Then the material was calcined at different temperatures, 500^{0}C and 950^{0}C. After the furnace is off, on cooling the oxygen is allowed to flow into the furnace at intervals (Oxygen Annealing). A final furnace temperature of 950^{0}C is maintained after the intermediate firings. Higher temperature than this will result in a material that is much harder to regrind. Temperatures above 1050^{0}C may destroy the crystal structure. Then X-ray diffraction spectrum of these materials was taken. For experimental conformation calculated particle size value, Scanning Electron Microscopy (SEM) photograph was taken. The composition details of the prepared ceramics were determined from EDX.

2.1. XRD Analysis.

X-ray Diffraction pattern for the three different temperatures in steps for the sample $La_{0.1}ZrY_{0.9}BaCa_2Cu_3O_{4.5}$ was taken using Bruker AXS D8 advance diffractometer (figure 2). The diffractometer with radiations of wavelength 1.54184Å having Nickel filter, equipped with X-ray generator 1140/90/96 having X-ray source KRISTALLOFLXE 780,KF,4KE with wide angle goniometer PW1710/70 with single pen recorder pm 8203 and channel control PW1390 at 35kV, 10mA is used for the purpose. The scanning speed of the specimen is 2 degree/minute. From the XRD results, the obtained d values compared with the JCPDS (Joint Committee on Powder Diffraction Standards) file values[10,11] and XPERT PRO programme was applied. So it can be concluded that this crystal is found to be orthorhombic system:

a=15.3598, b=11.1644, c=3.3835: $\alpha=\beta=\gamma=90^0$

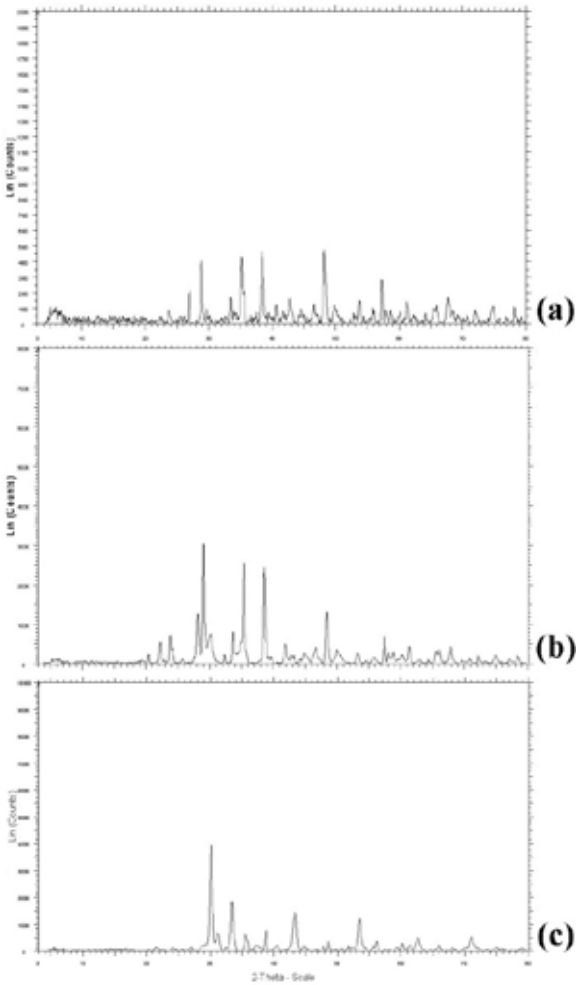

Figure.2 XRD of $La_{0.1}ZrY_{0.9}BaCa_2Cu_3O_{4.5+x}$ at temperatures: (a)900^{0}C (b)500^{0}C (c)30^{0}C.

Using Debye Scherrer equation the particle size of $La_{0.1}ZrY_{0.9}BaCa_2Cu_3O_{4.5+x}$ calculated from the XRD results. Here the authors studied the variation of XRD spectrum of $La_{0.1}ZrY_{0.9}BaCa_2Cu_3O_{4.5+x}$ at different treating temperatures.

2.2. Particle size measurements.

Crystal structures were solved by analyzing the intensities of diffracted X-ray beams. X-ray diffraction profile were used to measure the average crystal size in the sample provided the average diameter is less than 200Å. The lines in a powder diffraction pattern are of finite breadth but if the particles are very small, the lines are broaden than usual. The broadening decreases with the increase in particle size. The particle size for $La_{0.1}ZrY_{0.9}BaCa_2Cu_3O_{4.5+x}$ was calculated from X-ray diffraction profiles of strong reflections with intensity % by measuring the full width at half maximum (FWHM). The Debye Scherrer equation for calculating the particle size is given by [3,8]

$$D = \frac{K\lambda}{\beta\cos\theta}$$

Where K is the Scherrer constant, λ is the wavelength of light used for the diffraction, β is the 'full width at half maximum' of the sharp peaks, and θ is the angle measured. The Scherrer constant (K) accounts for the shape of the particle and is generally taken to have the value 0.9. The results revealed that the particle size is 25nm. The particle sizes of $La_{0.1}ZrY_{0.9}BaCa_2Cu_3O_{4.5+x}$ of different temperature are shown in the Table1.

Table:1 The particle size of $La_{0.1}ZrY_{0.9}BaCa_2Cu_3O_{4.5+x}$ at different temperatures, calculated by Debye Scherrer formula.

Data of high intensity peak of XRD at different temperatures	θ (radian)	β(radian) ($x10^{-3}$)	Particle size (nm)
$La_{0.1}ZrY_{0.9}BaCa_2Cu_3O_{4.5+x}$ 30^{0}C	0.2628	7.2605	19.1124
$La_{0.1}ZrY_{0.9}BaCa_2Cu_3O_{4.5+x}$ 500^{0}C	0.2529	6.0563	22.9128
$La_{0.1}ZrY_{0.9}BaCa_2Cu_3O_{4.5+x}$- 900^{0}C	0.4209	4.0491	34.2711

2.3. XRD-Instrumental Broadening.

Appreciable broadening in X-ray diffraction lines will occur When particle size is less than 100nm. Diffraction pattern will show broadening because of particle size and strain. The observed line broadening was used to estimate the average size of the particles. The total broadening of the diffraction peak is due to sample and the instrument. The sample broadening is described by

$$FW(s) \times \cos\theta = \frac{K\lambda}{size} + 4 \times strain \times \sin\theta$$

The total broadening β_t equation is described by

$$\beta_t^2 \approx \left\{\frac{0.9\lambda}{D\cos\theta}\right\}^2 + (4\varepsilon\tan\theta)^2 + \beta_0^2$$

Where D is average particle size, ε is strain and β_o is instrumental broadening. Instrumental broadening is presented in Figure.3.

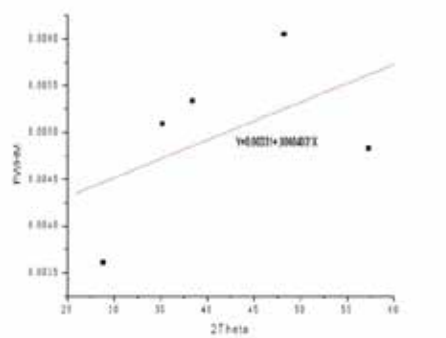

Figure.3. Typical Instrumental Broadening

2.4. Williamson-Hall Plot.

It relies on the principle that the approximate formulae for size broadening, β_L, and strain broadening, β_e , vary quite differently with respect to Bragg angle, θ. This method is attributed to G.K.Williamson and his student, W.H.Hall. Williamson and Hall proposed a method for deconvoluting size and strain broadening by looking at the peak width as a function of 2θ[5].

$$\beta_L = \frac{K\lambda}{L\cos\theta}$$

$$\beta_e = C\varepsilon\tan\theta$$

One contribution varies as tanθ and the other as 1/cosθ . If both contributions are present then their combined effect should be determined by convolution. The simplification of Williamson and Hall is to assume the convolution is either a simple sum or sum of squares. Using the former equations, we get:

$$\beta_{tot} = \beta_e + \beta_L = C\varepsilon\tan\theta + \frac{K\lambda}{L\cos\theta}$$

If we multiply this equation by cosθ we get:

$$\beta_{tot}\cos\theta = C\varepsilon\sin\theta + \frac{K\lambda}{L}$$

Volume : 3 | Issue : 12 | December 2014 • ISSN No 2277 - 8179

and comparing this to the standard equation for a straight line (m = slope; c = intercept) y = mx + c.

By plotting $\beta_{tot}\cos\theta$ versus $\sin\theta$ we obtained the strain component from the slope ($C\varepsilon$) and the size component from the intercept ($K\lambda/L$). Such a plot is known as a Williamson-Hall Plot. However the Williamson-Hall method has many assumptions: its absolute values should not be taken too seriously but it can be a useful method if used in the relative sense; for example a study of many powder patterns of the same chemical compound, but synthesized under different conditions, might reveal trends in the crystallite size/strain which in turn can be related to the properties of the product. Figure.4 illustrates the Williamson Hall Plot.

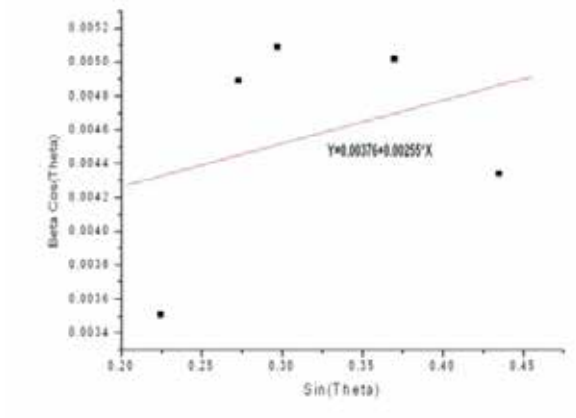

Slope=0.004282, Y intercept=0.004266
Correlation coefficient=0.31943
Standard deviation of the fit=$7.2412\text{x}10^{-4}$
Figure.4. Williamson Hall Plot.

2.5. SEM Analysis.
Morphology has been analyzed from Scanning Electron Microscope (SEM). The SEM analyses the surface of solid objects, producing images of higher resolution than optical microscopy. It produces representations of three dimensional samples from a diverse range of materials. Figure.5 is the surface morphology of $La_{0.1}ZrY_{0.9}BaCa_2Cu_3O_{4.5\ at\ 950oC.}$ The particle size measurement through SEM revealed its maximum dimensions always less than 100nm [9] .

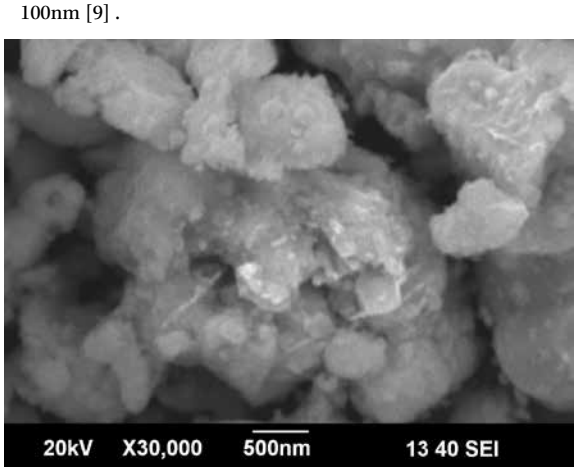

Figure.5 SEM photograph of $La_{0.1}ZrY_{0.9}BaCa_2Cu_3O_{4.5+x}$

2.6. Energy Dispersed X-ray Spectrograph (EDX). EDX (figure.6) gave the composition details of the prepared ceramic powder at 950°C. ISIS Link Oxford Instrument UK is used for this measurement. This technique generally associated with Scanning Electron Microscope (SEM) and in this technique an electron beam of 10-20 KeV strikes the surface of a sample which causes X-ray to be emitted from point of incidence. Here, the energy of the X-ray emitted depends on material under examination. The energy of the characteristic X-ray emitted from the different elements is different and thus it gives the unavoidable signature of the particular element corresponding to particular value. When an X-ray strikes the detector, it will generate a photoelectron which in turn generates electron-hole pairs[7]. A strong electric field attracts the electrons and holes towards the opposite ends of the detector. The size of the pulse thus generated depends on the number electron-hole pairs created, which in turn depends on the energy of the incoming X-ray. In this method however elements with low atomic number are difficult to be detected. The detector which is Lithium doped Silicon (SiLi) is protected by a Beryllium window and operated at liquid Nitrogen temperatures. The absorption of the soft X-rays by the Beryllium decreases the sensitivity below an atomic number of 11[7] .

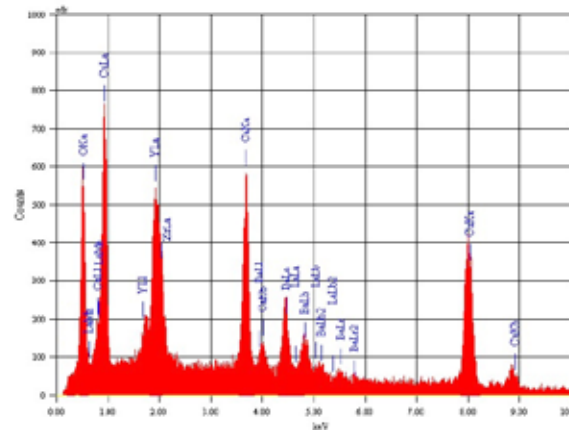

Figure.6. EDX of $La_{0.1}ZrY_{0.9}BaCa_2Cu_3O_{4.5+x.}$

3. Results and Discussion
In Figure.2 the XRD patterns of $La_{0.1}ZrY_{0.9}BaCa_2Cu_3O_{4.5+x}$ powder obtained for various annealing temperatures are shown. XRD spectrum for the different temperatures gave a clear idea about the maximum intensity peak shifting corresponds to the different treating temperatures as shown in the figure. And also get the maximum intensity peak difference. As the temperature increases, the highest peaks in the XRD spectrums shifts from left to right through the 2θ axis and the highest intensity peak decreases.

The atoms undergo thermal vibration about their mean positions even at the absolute zero of temperature, and the amplitude of this vibration increases as the temperature increases. As the result of an increase in temperature, thermal vibration of the atoms Increased, the unit cell expands, causing changes in plane spacing d and therefore in the 2θ positions of the diffraction lines. And also the intensities of the diffraction lines decrease.

When a prepared material heated from room temperature to high temperature, the amplitude of the thermal vibrations increased. The amplitude is very higher than that at room temperature. After heating, the material cooled to room temperature. The amplitude of the atomic vibrations of the material was decreased. But it couldn't arrive at the initial amplitude. The atomic vibration amplitude of the heated material was higher than initial amplitude. That means, the atomic vibration amplitude increases, the intensity of the diffracted beam also decreases because it has the effect of smearing out lattice planes. This reinforcement requires that the path difference, which is a function of the plane spacing d, between waves scattered by adjacent planes be an integral number of wavelengths. Thus the reinforcement of waves scattered at the Bragg angle by various

parallel planes is not as perfect as it is for a crystal with their fixed atoms. The thickness of the planes is 2u, where u is the average displacement of an atom from its mean position. Under these conditions reinforcement is no longer perfect, and it becomes more imperfect as the ratio u/d increases, i.e., as the temperature increases since that increases u, or as θ increases, since high- θ reflections involve planes of low d value. Thus the intensity of a diffracted beam decreases as the temperature is raised. In intensity calculations, the temperature factor e^{-2M} decreases as 2θ increases [6].

Figure.2 indicates, the peak broadening in the XRD patterns clearly indicated the nature of the nano crystals. From the width of the XRD peak, the mean crystalline size can be calculated using Debye Scherrer's equation. From Table.1, particle size of the material $La_{0.1}ZrY_{0.9}BaCa_2Cu_3O_{4.5}$ increases with respect to the treating temperature increasing. It is realized that, θ increases with temperature. The results revealed that the particle size is less than 100nm.The diffraction data revealed that the material belongs to orthorhombic symmetry with a=15.3598, b=11.1644, c=3.3835: $\alpha=\beta=\gamma=90^0$. The XRD results were compared with JCPDS data and applied the XPERT PRO software.

Heat treatment causes the particles of the sample to anneal and form larger grains, which of course indicates that the particles become larger. Hence, the large particle size of sample at 950°C is expected. This also agrees with the

100nm. This is an experimental proof of the theoretical calculation of particle size by Debye Scherrer equation from XRD data.

EDX spectrum of $La_{0.1}ZrY_{0.9}BaCa_2Cu3O_{4.5+x,}$ gave the information on the elemental composition of the material. The elemental compositions agree with the stoichiometric relations of the prepared compound. The EDX spectrums obtained (figure.6) give the material higher crystallinity, as having larger grains means more long-range order, and hence more crystallinity[1,2].

Figure.5 shows SEM image of $La_{0.1}ZrY_{0.9}BaCa_2Cu3O_{4.5+x,}$ The SEM photograph revealed maximum dimensions of the particles to be always less than composition of the sample under investigation at 950°C.

Table 2. Material Content (EDX)

Material	content(%)
La	16.97
Zr	2.13
Y	20.49
Ba	9.5
Ca	10.9
Cu	32.59
O	7.44

From the EDX spectrum, the dominant peak positions at, 0.833kev, 4.650kev, 2.042kev, 1.922kev, 4.465kev, 3.690kev, 0.930kev, 8.040keV, 0.525keV correspond quite well to the energy pattern of the corresponding materials (LaM, LaLα, ZrLα, YLα, BaLα, CaKα, CuLα, CuKα and OKα) reported in the EDAX international chart, giving the evidence that La Y& Cu are dominant in $La_{0.1}ZrY_{0.9}BaCa_2Cu3O_{4.5+x}$ samples. Table.2, shows the percentage of the elements in the prepared $La^{0.1}ZrY_{0.9}BaCa_2Cu3O_{4.5+x}$sample.

When, particle size becomes smaller, due to size effect, the peaks become broad and widths larger. The size and strain of the experimentally observed broadening of several peaks are computed simultaneously using *least squares method*. The broadening of peak may also occur due to micro strains of the crystal structure arising from defects like dislocation and twinning [4].

In this investigation, Williamson-Hall plot is plotted with sin θ on the x-axis and βcosθ on the y-axis (in radians). A linear fit is got for the data. From this fit, particle size and strain are extracted from y-intercept and slope respectively. The extracted particle size is 32.528 nm and strain is 0.00522 from Williamson Hall Plot (Figure.4).

4. Conclusion

In this work $La_{0.1}ZrY_{0.9}BaCa_2Cu3O_{4.5+x,}$ ceramics were prepared successfully by the conventional solid state reaction technique and Characterized by XRD, SEM, EDX, and particle size measurement. XRD data confirmed the formation of the perovskite phase structure and the average particle size. The XRD spectrums of the $La_{0.1}ZrY_{0.9}BaCa_2Cu3O_{4.5+x,}$at different temperatures indicate that, according to increasing treating temperature, the θ value and particle size also increases. From SEM analysis, the morphology images clearly show the approximate size of the nano particles. The value of particle size calculated from the Williamson-Hall plot method is in agreement with that of the particle size measured from Debye Scherrer formula of the sample. The EDX analysis indicates that the elements existing in the sample and it agree with the nonstoichiometric relations of the prepared compound.

Acknowledgement

The authors are thankful to UGC, Kerala State Council For Science, Technology And Environment (KSCSTE), Thiruvanathapuram for granting the financial assistance, SAIF, Kochi for providing the instrumental data and to the Principal, CMS College, Kottayam, Kerala for providing the facilities.

REFERENCE

[1] W.W. So, J. S. Jang,Y. W. Rhee, K. J. Kim, S.J. Moon, (2001 "Preparation of Nanosized Crystalline CdS Particles by the Hydrothermal Treatment", Journal of Colloid and Interface Science, Vol. 237, No. 1,) pp. 136-141. | [2]Q. Xie, F. McCourt, (2008) Nanotechnology Engineering NE 320L Lab Manual, University of Waterloo, Waterloo, pp 35-39. | | [3] A.R. West, (1974). " Solid State Chemistry | and It's Applications",Wiley,New York. | | [4] S. C. Ghosh and C.Thanachayanont, J.Dutta, (2004), "Studies on Zinc sulphide nanoparticles for Field Emission Devices". The 1st ECTI Annual Conference (ECTI-CON2004), Pattaya, Thailand, 13-14 pp.145-148. | [5] G. K. Williamson, W.H. Hall, (1953) "X-ray Line Broadening from filed Aluminium and Wolfram", Acta Metallurgica, Vol. 1, , pp. 22-31. | [6]B. D. Cullity, (1978) "Elements of X-ray Diffraction",2nd Edition Addison-Wesley Publishing Company.Inc., | Phillippines. | [7]Sharath S N K, Nandakumar S H; (2005) | "Resonance" 10, 61 | [8]Glatter O, Krathy O; (1982) "Small angle | X ray scattering", Academic press | London. | [9]Babu TGN, Warrier PRS, Damodaran | A.D; (1997)"material science" 32 1759. | [10]Zhang Y, Cheng YB, Lathabhai S, Hiaro K; | (2005) "J American ceramic | society" 88 114. | [11]Hameed N, Thomas S.P, Abraham R, | Thomas S; (2007) "exp. Poly Lett 1, 345. |